

## Ideal performance of a self-cooling greenhouse

Davies, Philip A.; Zaragoza, Guillermo

DOI:

[10.1016/j.applthermaleng.2018.12.056](https://doi.org/10.1016/j.applthermaleng.2018.12.056)

License:

Creative Commons: Attribution-NonCommercial-NoDerivs (CC BY-NC-ND)

*Document Version*

Peer reviewed version

*Citation for published version (Harvard):*

Davies, PA & Zaragoza, G 2019, 'Ideal performance of a self-cooling greenhouse', *Applied Thermal Engineering*, vol. 149, pp. 502-511. <https://doi.org/10.1016/j.applthermaleng.2018.12.056>

[Link to publication on Research at Birmingham portal](#)

**Publisher Rights Statement:**

Checked for eligibility: 19/12/2018

**General rights**

Unless a licence is specified above, all rights (including copyright and moral rights) in this document are retained by the authors and/or the copyright holders. The express permission of the copyright holder must be obtained for any use of this material other than for purposes permitted by law.

- Users may freely distribute the URL that is used to identify this publication.
- Users may download and/or print one copy of the publication from the University of Birmingham research portal for the purpose of private study or non-commercial research.
- User may use extracts from the document in line with the concept of 'fair dealing' under the Copyright, Designs and Patents Act 1988 (?)
- Users may not further distribute the material nor use it for the purposes of commercial gain.

Where a licence is displayed above, please note the terms and conditions of the licence govern your use of this document.

When citing, please reference the published version.

**Take down policy**

While the University of Birmingham exercises care and attention in making items available there are rare occasions when an item has been uploaded in error or has been deemed to be commercially or otherwise sensitive.

If you believe that this is the case for this document, please contact [UBIRA@lists.bham.ac.uk](mailto:UBIRA@lists.bham.ac.uk) providing details and we will remove access to the work immediately and investigate.

# Ideal performance of a self-cooling greenhouse

Philip A. Davies<sup>1\*</sup> and Guillermo Zaragoza<sup>2</sup>

1. Sustainable Environment Research Group, School of Engineering and Applied Science, Aston University, Birmingham, B4 7ET, UK
2. CIEMAT, Plataforma Solar de Almería, Ctra. de Senés s/n, 04200 Tabernas, Almería, Spain

\* p.a.davies@bham.ac.uk

**Abstract:** The self-cooling greenhouse is a concept to enable crop cultivation in adversely hot climates. It sacrifices a fraction  $\gamma$  of the incident solar energy to drive a refrigeration system, thus lowering the internal temperature below ambient. Heat is actively rejected to a stream of coolant such as air or water. To maintain availability of sunlight for photosynthesis,  $\gamma$  should be as small as possible. Nonetheless, the laws of thermodynamics dictate a minimum value of  $\gamma$ . Using the approach of endoreversible thermodynamics and the theory of selective blackbody absorbers, we determine ideal minimum values achievable for cases of both thermal and photovoltaic solar collection with and without solar concentration. To achieve an internal temperature 10°C below that of the incoming coolant, a minimum  $\gamma=0.056$  is needed using multicolour absorption at maximum concentration  $C=46300$  – representing an absolute minimum for either type of solar collection. Without concentration ( $C=1$ ) a selective thermal collector permits minimum  $\gamma=0.089$  and a single-junction PV solar collector permits minimum  $\gamma=0.15$ . We discuss briefly implications for development of a real self-cooling greenhouse to approximate the performance of these ideal cases.

**Keywords:** Solar refrigeration; greenhouse cooling; solar thermal; solar PV; thermodynamic limit; endoreversible.

38 **Nomenclature**

39

Symbol	Unit	Description
$A$	$m^2$	Area of PV cell or thermal receiver
$c$	$m\ s^{-1}$	Speed of light in a vacuum
$c_p$	$J\ kg^{-1}\ K^{-1}$	Specific heat capacity of coolant at constant pressure
$C$		Concentration ratio
$COP$		Coefficient of performance
$E$	eV	Energy level of photon
$E_g$	eV	Bandgap
$f$		Solar dilution factor
$h$	J s	Planck's constant
$k$	$J\ K^{-1}$	Boltzmann constant
$m$	$kg\ s^{-1}$	Mass flow of coolant
$N$	$s^{-1}$	Net rate of photon absorption by PV cell
$q$	$eV\ V^{-1}$	Elementary charge ( $q=1$ )
$Q_h$	W	Heat flow from solar collector to refrigerator
$\delta Q_i$	W	Heat flow from $i$ 'th solar collector
$Q_{int}$	W	Heat flow from interior of greenhouse to refrigerator
$Q_{sun}$	W	Radiative heat flow from sun to greenhouse
$T_{c1}$	K	Temperature of coolant at inlet
$T_{c2}$	K	Temperature of coolant at inlet
$T_{cell}$	K	Temperature of PV cell
$T_h$	K	Temperature of solar collector
$T_i$	K	Temperature of the $i$ 'th collector
$T_{int}$	K	Temperature of interior of greenhouse
$T_{sky}$	K	Effective temperature of sky
$T_{sun}$	K	Effective temperature of Sun
$\bar{T}$	K	Log mean temperature
$V$	V	Bias voltage of PV cell
$W$	W	Work done by the solar cell
$\gamma$		Fraction of greenhouse shaded by solar collector
$\eta$		Efficiency of solar collection or conversion
$\lambda$		Fraction of solar radiation thermalized by PV cell

40

41 Note since  $E$  is measured in eV and  $Q_{sun}$  in watts, a conversion factor of  $1.602 \times$   
 42  $10^{-19}$  J/eV is applied after use of  $E$  and  $E_g$  in Planck's law in the numerical  
 43 calculations.

44

45

46 **Abbreviations**

47

48 COP Coefficient of performance

49 PV Photovoltaic

50

51

## 52 1. Introduction

53

54 Increasing ambient temperatures and growing populations require new methods  
55 for cultivation of crops under adverse conditions. Global temperatures from  
56 2013-2017 showed the highest five-year average on record <sup>1</sup>. In many instances,  
57 regions having some of the hottest climates are also experiencing exceptionally  
58 fast population growth; for example, Pakistan, Egypt and Somalia are expected to  
59 see population increase by 24%, 27% and 46% respectively between 2017 and  
60 2030 compared to the global average of only 14% over the same period <sup>2</sup>. The  
61 vulnerability of such populous and agriculturally-dependent countries to  
62 changing climate is a serious cause for concern <sup>1</sup>.

63

64 Protected cultivation of crops within greenhouses is a way to maintain and  
65 increase crop yields despite climate variability. Unlike in open-field cultivation,  
66 conditions can be kept at desired levels by heating and cooling systems. In hot  
67 climates, cooling is needed, for which a number of technologies have been  
68 proposed or are already in use. These include shading, ventilation, earth-to-air  
69 heat exchangers, fogging, and evaporative cooling with pad-and-fan systems <sup>3,4</sup>.

70

71 Evaporative cooling is currently the preferred technology for greenhouse cooling  
72 in hot climates; but its performance is limited, especially under humid  
73 conditions, as it cannot cool below the wet-bulb temperature <sup>5</sup>. Lower  
74 temperatures are achievable using vapour compression refrigerators <sup>6,7</sup>.

75 Nonetheless, such refrigerators use excessive energy when scaled up to the  
76 multi-hectare installations common in commercial crop production. Use of  
77 conventional energy resources for greenhouse cooling by vapour compression  
78 refrigerators, or by other active systems, would be unlikely to provide a  
79 sustainable solution for crop production in coming years. Since, however, solar  
80 energy is naturally abundant at locations and times of year where cooling is most  
81 needed, it makes sense to investigate cooling of greenhouses powered by the  
82 sun.

83

84 The challenge in any solar-powered cooling is the large solar collection area  
85 potentially required, which could increase markedly the footprint of a  
86 greenhouse. For example, Puglisi, et al. <sup>8</sup> developed a solar-powered absorption  
87 refrigeration to cool a greenhouse in Italy, for which they required an area of  
88 solar collector comparable in size to the greenhouse itself. Lychnos and Davies <sup>9</sup>  
89 investigated the feasibility of greenhouse cooling by means of a solar-powered  
90 liquid desiccant cycle with an open collector-regenerator. Depending on location  
91 and ambient conditions, the collector-regenerator was predicted to occupy 0.5 to  
92 4.5 times the greenhouse plan area.

93

94 In this study, we propose that it would be advantageous to devise a greenhouse  
95 cooling system whereby the solar energy collection is compactly integrated into  
96 the greenhouse, without occupying any external footprint. If realised, such a  
97 concept could be termed a *self-cooling greenhouse*. The challenge for the design  
98 of the self-cooling greenhouse is whether it can be made efficient enough to  
99 achieve low temperatures without robbing the plants of incoming solar energy  
100 such as to slow down growth and decrease crop yield significantly.

101 With the motivation of minimising the total footprint of energy production and  
102 agriculture, numerous researchers modelled and developed the integration of  
103 solar collectors (especially photovoltaic, PV, type) with greenhouse structures  
104 and cladding<sup>10-15</sup>. As in the current study, some have investigated the degree of  
105 shading created by the solar collectors and how this affects overall feasibility.  
106 The studies are not limited to small prototypes but include commercial-scale  
107 installations. Pérez-Alonso et al.<sup>13</sup>, for example, constructed and monitored a  
108 1024 m<sup>2</sup> pilot greenhouse incorporating amorphous silicon solar cells externally  
109 fixed to the greenhouse cover, shading 9.72% of the roof area in a checkerboard  
110 pattern. Hassanien et al.<sup>15</sup> evaluated building-integrated crystalline PV cells  
111 comparing them against conventional greenhouse cladding in greenhouses of 26  
112 m<sup>2</sup> footprint. With 20% shading, they observed no significant loss of yield in a  
113 tomato crop. Castellano et al.<sup>16</sup> reported a 500 m<sup>2</sup> greenhouse installation in  
114 which the roof was entirely obscured by crystalline solar PV panels, with light  
115 entering by the side walls only. They studied the photon flux both numerically  
116 and experimentally, though did not report on the crop yield. Micro-spherical  
117 crystalline silicon PV-cells have also been used, sandwiched between glass panes  
118 constituting the greenhouse cladding.<sup>14</sup> Similar micro-spherical cells have been  
119 used in venetian blind arrangements, in a prototype greenhouse of 24 m<sup>2</sup> floor  
120 area<sup>17,18</sup>. Instead of silicon, Emmott, et al.<sup>19</sup> proposed using organic PV,  
121 highlighting its potential for selective light absorption and low cost. Allardyce, et  
122 al.<sup>20</sup> highlighted the potential of dye-sensitized cells for selective absorption and  
123 increased biomass yield. Dupraz, et al.<sup>21</sup> calculated that the integration of  
124 photovoltaics with greenhouses can make better overall use of land, compared to  
125 when agricultural and energy harvesting are kept separate. Nonetheless, the  
126 above researchers considered the integration of solar PV for electricity  
127 production mainly, and not specifically for active greenhouse cooling.

128  
129 In a self-cooling greenhouse, the amount of sunlight sacrificed for refrigeration  
130 should be minimized – because the light is needed for photosynthesis primarily.  
131 According to Marcelis, et al.<sup>22</sup>, reduction in light intensity by 1% generally  
132 results in a reduction in yield of between 0.7 and 1% for greenhouse crops. The  
133 exact relation depends on a number of factors e.g. the species, CO<sub>2</sub> concentration,  
134 spectral composition of the light, temperature, and nutrient levels<sup>23</sup>. At higher  
135 light levels, the sensitivity of yield with respect to intensity is generally  
136 decreased, because of the limiting effect of other factors such as CO<sub>2</sub>  
137 concentration<sup>23,24</sup>. Aggregated data showed that a 33% reduction in light  
138 intensity (starting from 6 kWh/m<sup>2</sup>.day) resulted in a 20% average reduction in  
139 the yield of cucumber<sup>22</sup>. This suggests that the sacrifice of light should be <30%  
140 approximately for good crop yield to be maintained.

141  
142 A self-cooling greenhouse will need to reject heat to the surroundings. For this  
143 purpose, a cooling fluid (coolant) will be required as a heat sink. Most likely this  
144 fluid will be water or air. Water is an excellent coolant due its high heat capacity  
145 and thermal conductivity. Thus in coastal locations, seawater appears to be an  
146 attractive coolant, as it is abundantly available. Elsewhere, water from aquifers  
147 or rivers might be used. A preliminary calculation shows that the flow of water  
148 (or other fluid) tends to be large. For example, a 1 hectare greenhouse receiving  
149 1 kW/m<sup>2</sup> of solar irradiance generates a heat load of approximately 10 MW,

150 enough to heat a stream of water flowing at 0.25 m<sup>3</sup>/s by about 10°C. To  
151 minimize capital and operating costs of associated pipeline construction and  
152 pumping, it is therefore desirable that this flow be kept to a minimum for a given  
153 target temperature inside the greenhouse.

154

155 Using generalised assumptions about the cooling fluid and other aspects, this  
156 paper considers the feasibility of a self-cooling greenhouse from a fundamental  
157 thermodynamic perspective. To the authors' knowledge, such a fundamental  
158 study has not been undertaken. To address the gap, this paper aims to establish  
159 the ideal limits to performance based on the laws of thermodynamics. Typical  
160 design objectives for a self-cooling greenhouse would be to:

- 161 i. Achieve a substantial temperature drop (say 15°C) inside the greenhouse  
162 relative to ambient
- 163 ii. Incur minimum sacrifice of light (say <30%) in driving the refrigeration  
164 process
- 165 iii. Require minimum flow of coolant to remove the heat.

166

167 These three objectives conflict; therefore it is important to quantify and  
168 understand the relations among them. This paper explores these relations by  
169 establishing ideal models of the self-cooling greenhouse, thus allowing the trade-  
170 offs among the design objectives to be investigated. The analysis sets out to be as  
171 general as possible, establishing limits according to general principles with  
172 minimal dependence on the technological designs and materials used. Such an  
173 idealised study is useful to provide a benchmark against which real systems or  
174 proposed design concepts can be evaluated.

175

176 The concept of an idealised performance based on thermodynamic principles is  
177 already well established in solar energy research. We could cite, for example, the  
178 works by Shockley and Queisser<sup>25</sup> and by Trivich and Flinn<sup>26</sup> on the limiting  
179 performance of PV cells, and the many subsequent works building on those (e.g.  
180 <sup>27-31</sup>). We could also cite comparable seminal works in the area of solar thermal  
181 energy conversion such as those of Castañs<sup>32</sup> and De Vos<sup>33</sup>. Although those  
182 works did not set out many technological details of specific devices, they gave  
183 general results that were very useful to guide practical developments of solar  
184 energy collection devices subsequently. Similarly it is hoped that the current  
185 study will guide development of future self-cooling greenhouses.

186

187 First we explain the concept and assumptions used in the analyses, then present  
188 the mathematical analyses themselves for different cases covering both thermal  
189 and PV collection. This is followed by a general analysis for the ultimate  
190 thermodynamic performance of an ideal self-cooling greenhouse. Sensitivity  
191 analyses are included to assess the effect of varying the baseline assumptions.  
192 Finally, we discuss briefly technologies and prospects for implementation of real  
193 systems intended to approximate the ideal limits in practice; and we propose  
194 topics for future study.

195

196

## 197 2. Concept and assumptions

198

199 As an idealized case, the self-cooling greenhouse is conceptualized as a box with  
200 a transparent and horizontal roof that transmits perfectly incident solar  
201 radiation, at the same time insulating against all convective and conductive heat  
202 transfer. The box includes a refrigeration system that rejects heat to a flowing  
203 stream of coolant (Fig. 1). The only loss in solar transmission is that  
204 corresponding to the fraction  $\gamma$  of energy diverted to the solar collector used to  
205 drive the refrigeration system. The remaining fraction  $(1-\gamma)$  is assumed to be  
206 absorbed entirely by the crops and soil inside the greenhouse – which behave as  
207 black body absorbers. The solar collector may be contained inside the  
208 greenhouse, or its surface may be integrated in the roof. It is assumed that the  
209 solar collector is completely opaque, such that  $\gamma$  equals the area fraction  
210 occupied geometrically by the collector.

211

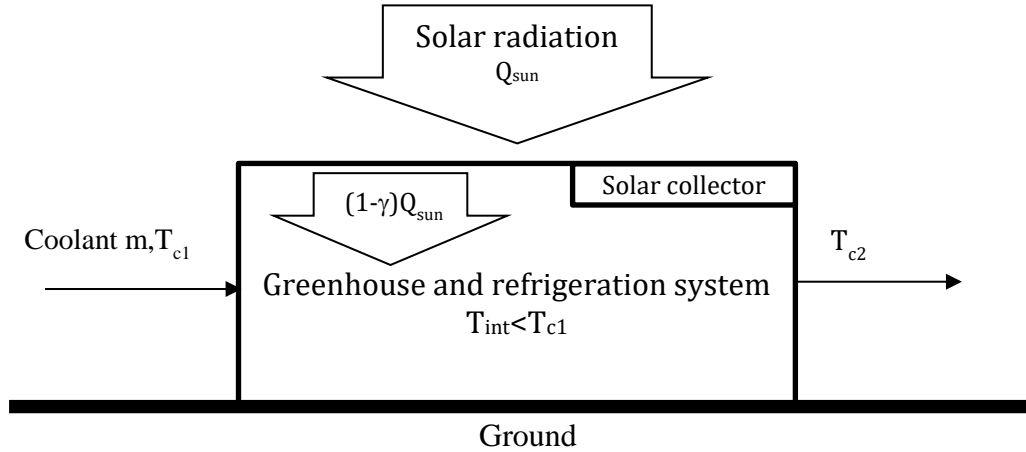
212 Like in many works aimed at determining the ideal performance of solar energy  
213 conversion processes (e.g. <sup>32,33</sup>), the sunlight is modelled as blackbody radiation.  
214 This assumption is justified since self-cooling greenhouses would most likely be  
215 used in sunny climates where relatively clear-sky conditions are common. It is  
216 also assumed that the radiation falls perpendicularly on the greenhouse roof,  
217 because this type of greenhouse would typically be used at low latitudes (10-  
218 35°). Approximately overhead sunlight and clear sky conditions will tend to  
219 coincide with the times of day and year when the cooling system is most needed,  
220 and thus represent the appropriate assumptions. Moreover, more specific  
221 assumptions would limit the study to whatever particular solar radiation  
222 conditions were chosen, resulting in a loss of generality.

223

224 Solar and heat gain through the side walls of the greenhouse are assumed  
225 negligible. This assumption is justified by the fact that the greenhouse is  
226 intended for production of bulk quantities of crops to improve food security, and  
227 as such should cover extensive areas (e.g. several hectares) such that the  
228 sidewalls are very small in area compared to the roof. The assumption also has  
229 the advantage of making the results independent of the size, orientation and  
230 geometry of greenhouse.

231

232 An initial assumption is that the long-wave radiative heat transfer between the  
233 greenhouse and sky is negligible. To justify this assumption, we note that  
234 effective sky temperatures are typically 5-20°C below ambient <sup>34,35</sup> and that a  
235 practical aim would be to cool the greenhouse by approximately similar  
236 amounts; therefore the interior temperature ( $T_{int}$ ) is likely to be fairly close to  
237 the sky temperature, resulting in a long-wave heat flux that is much less than the  
238 solar radiation flux of order 1000 W/m<sup>2</sup>. (This assumption will be further  
239 verified in the Discussion section). In contrast, radiative heat transfer from the  
240 solar collector to the sky is *not* neglected because, as will be seen, the collector  
241 may require to be operated at a temperature much higher than ambient (in the  
242 case of a thermal collector) or it may suffer inevitable radiative losses (in the  
243 case of a photovoltaic collector). Important constants and baseline values of the  
244 main parameters, as needed to initiate the analysis, are summarised in Table 1.



245  
246  
247  
248  
249  
250  
251  
252  
253  
254  
255  
256

**Figure 1:** Idealized self-cooling greenhouse with transparent insulative roof, housing a solar energy collector that powers a refrigeration system. Heat is removed from the system by a coolant (e.g. seawater) with mass flow  $m$ , entering the box at temperature  $T_{c1}$  and leaving at  $T_{c2} > T_{c1}$ . The greenhouse internal temperature  $T_{int}$  must be maintained below  $T_{c1}$ . To drive the cooling system requires a fraction  $\gamma$  of the incoming solar radiation  $Q_{sun}$  to be sacrificed to the solar collector. The goal is to minimise  $\gamma$ . The solar collector, shown here schematically as a single unit, could in practice be configured as several units distributed over the roof area of the greenhouse.

**Table 1:** Fixed and baseline parameters used in the analysis.

Parameter	Unit	Value	Notes
Effective Sun temperature, $T_{sun}$	K	5762	Approximating solar radiation as a blackbody <sup>36,37</sup> . Different authors have used slightly different values e.g. Castañs <sup>32</sup> used 5770 K.
Solar dilution factor, $f$		$2.16 \times 10^{-5}$	As used by De Vos <sup>36</sup> , referring to the solar irradiance reaching the Earth as a fraction of that at the Sun's surface. Different sources used slightly different values as indeed the distance between the Sun and Earth varies due to ellipticity of orbit causing $f$ to vary.
Coolant inlet temperature, $T_{c1}$	K	303	This value (30°C) is representative of a warm sea such as the Red Sea in July to September <sup>38</sup> .
Coolant outlet temperature, $T_{c2}$	K	313	Cooling water in coastal power stations typically returns to the sea with a 8-10°C increase in temperature, so a 10°C increase is assumed here <sup>39</sup> . A range of 300-380 K is also considered.
Target interior temperature, $T_{int}$	K	293	This value of 20°C represents benign conditions for cultivation of temperate or subtropical crops according to the species and cultivation regime <sup>40</sup> . A range of 280-310 K is also considered.
Sky temperature, $T_{sky}$	K	293	Sky temperature is typically below ambient <sup>34,35</sup> and taken here as approximately equal to $T_{int}$ . Values of $T_{int} \pm 10^\circ\text{C}$ are also considered in the sensitivity analysis.

257  
258



### 259 3. Approach

260

261 Because this is an idealized thermodynamic analysis, the natural starting point is  
262 to assume reversible processes that do not increase the entropy of the  
263 surroundings. However, collection of solar energy is not a reversible process,  
264 because a solar collector has to operate at a temperature below that of the sun to  
265 allow net heat transfer to occur. The term ‘endoreversible’ has been used to  
266 describe solar energy conversion in the sense that reversibility only applies  
267 *inside* the solar energy conversion process. Similarly the self-cooling greenhouse  
268 is considered to be an endoreversible machine<sup>36, 41</sup>. The internal processes of  
269 solar energy conversion and refrigeration are assumed reversible, without  
270 consideration being given for example to the sizing of components for heat  
271 transfer in the refrigeration cycle.

272

273 Many results have been presented for the idealized efficiency of solar energy  
274 converters of both thermal and photovoltaic (PV) types<sup>27, 29, 30, 33, 36</sup>. Typically,  
275 these studies present efficiency as a function of just two temperatures: (i) the  
276 sun temperature, and (ii) the planet or sink temperature which is typically  
277 assigned a nominal value of say 290 K or 300 K<sup>27, 32</sup>. This current study builds on  
278 these earlier works, by considering such idealized converters driving a perfect  
279 reversible heat pump to remove heat from a greenhouse. A new feature is the  
280 flow restriction in the coolant, which means that a single sink temperature for  
281 the system cannot be assumed. Both the input and output temperatures of the  
282 coolant are important, as well as the sun temperature, giving three main input  
283 temperatures to determine  $\gamma$ .

284

285 To make the analysis as general as possible, this study broadly follows the  
286 approach of De Vos<sup>36</sup>, in that it sets out to rely on a justifiably minimum number  
287 of input parameters and assumptions about the physical processes used, thus  
288 providing results that are as general as possible. Nonetheless, separate analyses  
289 are needed for the cases of solar thermal and solar photovoltaic conversion  
290 processes because of the fundamental physical differences between these two  
291 types of process. After considering the separate cases, we will present a general  
292 analysis to represent ultimate ideal performance applying to both.

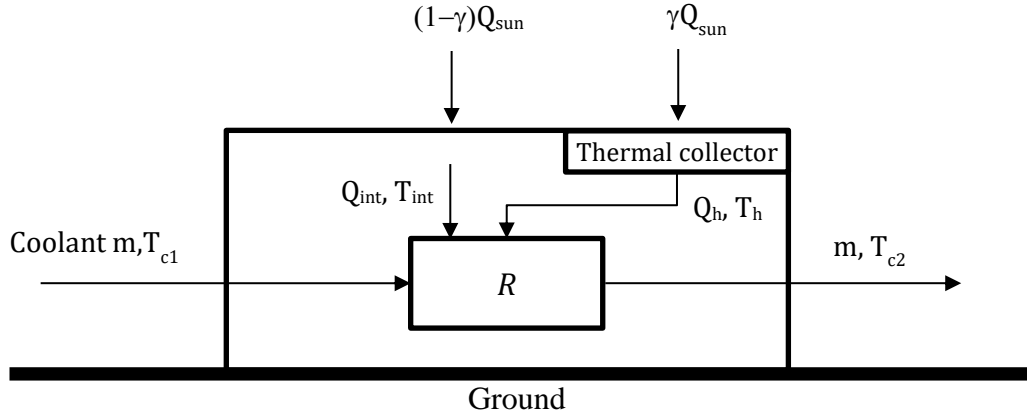
293

### 294 4. Case of solar thermal collector

295

296 For the case of the solar thermal collector, we include sub-cases with and  
297 without selective optical coating as used to reduce re-radiation of energy. For  
298 this case generally, we propose a thermally-driven refrigerator  $R$  that receives a  
299 driving heat flow  $Q_h$  [W] at temperature  $T_h$  [K] from the solar collector and  
300 absorbs heat  $Q_{int}$  [W] from the interior of the greenhouse at  $T_{int}$  (Fig. 2). A  
301 thermally-driven refrigerator could consist of a heat engine coupled  
302 mechanically to a heat pump; or it could use concepts based on vapour  
303 absorption cooling or liquid desiccant cooling, or on some other concept. Since  $R$   
304 is assumed reversible, however, we can ignore its internal mechanisms and  
305 consider only the entropy flows at its boundary, which must sum to zero.

306



307  
308

**Figure 2:** Case for the self-cooling greenhouse powered by a solar thermal collector delivering heat at rate  $Q_h$  to a reversible refrigerator  $R$ .

311  
312

Accordingly, the entropy balance gives:

313  
314

$$\frac{Q_h}{T_h} + \frac{Q_{int}}{T_{int}} = mc_p \ln \frac{T_{c2}}{T_{c1}} \quad (1),$$

316

and the enthalpy balance gives:

317  
318

$$Q_h + Q_{int} = mc_p(T_{c2} - T_{c1}) \quad (2)$$

320

where  $m$  [kg/s] is the mass flow of the coolant and  $c_p$  [kJ/kg K] is its specific heat capacity. The coolant has been assumed to be at constant pressure but, for nearly incompressible fluids like water, the equations remain valid even with moderate changes in pressure.

324  
325

Defining the coefficient of performance of the thermally-driven refrigerator as  $COP = Q_{int}/Q_h$ , we combine (1) and (2) to get:

326  
327  
328

$$COP = \frac{1 - \bar{T}/T_h}{\bar{T}/T_{int} - 1} \quad (3),$$

330

where  $\bar{T}$  is the logarithmic mean of  $T_{c1}$  and  $T_{c2}$ ,

331  
332

$$\bar{T} = \frac{T_{c2} - T_{c1}}{\ln(T_{c2}/T_{c1})} \quad (4).$$

334

Now  $Q_{int}$  is supplied by the solar radiation falling on the fraction  $(1-\gamma)$  of the greenhouse not shaded by the solar collector:

335  
336  
337

$$Q_{int} = (1 - \gamma)Q_{sun} \quad (5)$$

338

339

340 while  $Q_h$  is equal to the radiation falling on the solar collector (occupying fraction  
 341  $\gamma$  of the greenhouse roof area) multiplied by its efficiency  $\eta$ ,

$$342 \quad 343 \quad 344 \quad Q_h = \eta \alpha Q_{sun} \quad (6).$$

345 Combining eqs (5) and (6) with the definition  $COP = Q_{int}/Q_h$  and re-arranging  
 346 gives an expression for the minimum fraction of shading needed for the  
 347 greenhouse to be self-cooling:

$$348 \quad 349 \quad 350 \quad \gamma = \frac{1}{\eta COP + 1} \quad (7).$$

351 The calculation of  $\eta$  depends on the type of solar collector used.

#### 352 353 *4.1 Solar thermal collector without selective coating*

354 In this case the collector is considered a perfect blackbody, insulated from the  
 355 surroundings such that convective or conductive losses are avoided.

356 Nonetheless, there must occur radiation losses from the collector back to the  
 357 surroundings as noted by several authors (e.g. Castaños<sup>32</sup>, De Vos<sup>36</sup>, Müser<sup>42</sup>).

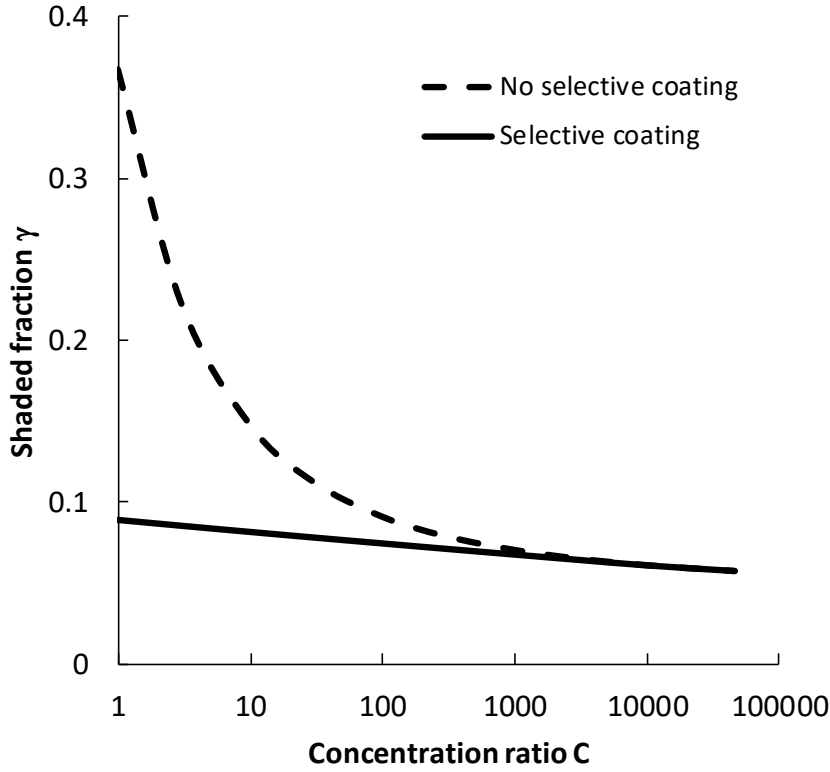
358 For a simple black-body collector the maximum efficiency is accordingly<sup>36</sup>:

$$359 \quad 360 \quad 361 \quad \eta = 1 - \frac{[T_h^4 - (1 - Cf)T_{sky}^4]}{CfT_{sun}^4} \quad (8).$$

362 As well as including bidirectional radiation exchange with the sun, the  
 363 expression includes radiation exchange with the sky at temperature  $T_{sky}$  and it  
 364 allows for the possible use of a concentrator, such as a mirror or lens, which  
 365 reduces the area of the receiver by a factor  $C$  for a given area over which sunlight  
 366 is collected. The area  $A$  of solar collection remains equal to  $\gamma$  multiplied by the  
 367 roof area of the greenhouse, with the aperture of the concentrating lens or  
 368 mirror occupying  $A$ . The concentrator is assumed to be lossless.

369 Thus  $\gamma$  can be determined from eqs. 3,4,7 and 8, given the input parameters  $T_{c1}$ ,  
 370  $T_{c2}$ ,  $T_{sun}$ ,  $T_{sky}$ ,  $f$  and  $C$ . As regards  $T_h$ , this has to be optimized to maximize the  
 371 product  $\eta COP$ , as  $COP$  increases with  $T_h$  while  $\eta$  decreases. (See Appendix B for  
 372 details of the optimization method). For  $C=1$  (no concentration) this results in  
 373  $T_h=365.5$  K (92°C),  $\eta=0.56$ ,  $COP=3.07$ , and  $\gamma=0.367$  (Table 2). Considering that  
 374 the real value of  $\gamma$  is likely to be substantially larger than this ideal minimum, this  
 375 simple black body collector seems quite unpromising as it is likely to end up  
 376 shading a large fraction (perhaps the entirety) of the greenhouse roof area. As  
 377 shown in Fig. 3,  $\gamma$  decreases with increasing  $C$  until a theoretical minimum of  
 378  $\gamma=0.0571$  occurs at  $C=46300$ . The corresponding collector temperature is  
 379  $T_h=2479$  K (2206°C).

380  
 381  
 382



383  
 384 **Figure 3:** Minimum fraction  $\gamma$  of greenhouse shaded by solar collector decreases with  
 385 solar concentration ratio  $C$ , with more marked dependence in the case where no  
 386 selective coating is used to decrease long-wave radiative losses. At maximum  
 387 concentration ( $C=46300$ ) the curves converge to  $\gamma=0.057$  for cases with and without  
 388 coating.

389  
 390 *4.2 Solar thermal collector with selective coating*

391  
 392 Selective optical coatings have long been used to improve the performance of  
 393 solar thermal collectors. Following Castañs<sup>32</sup> the analysis for this case considers  
 394 the solar radiation in two bands either side of a defined band gap  $E_g$ . For photons  
 395 with energy  $E < E_g$  there is no exchange of radiative energy between the sun (or  
 396 sky) and the collector; while for photons with  $E \geq E_g$  there is full exchange of  
 397 black body radiation. Thus the net solar energy collected is given by the  
 398 integration of Planck's law such that the collector efficiency for use in eq.(7)  
 399 becomes:

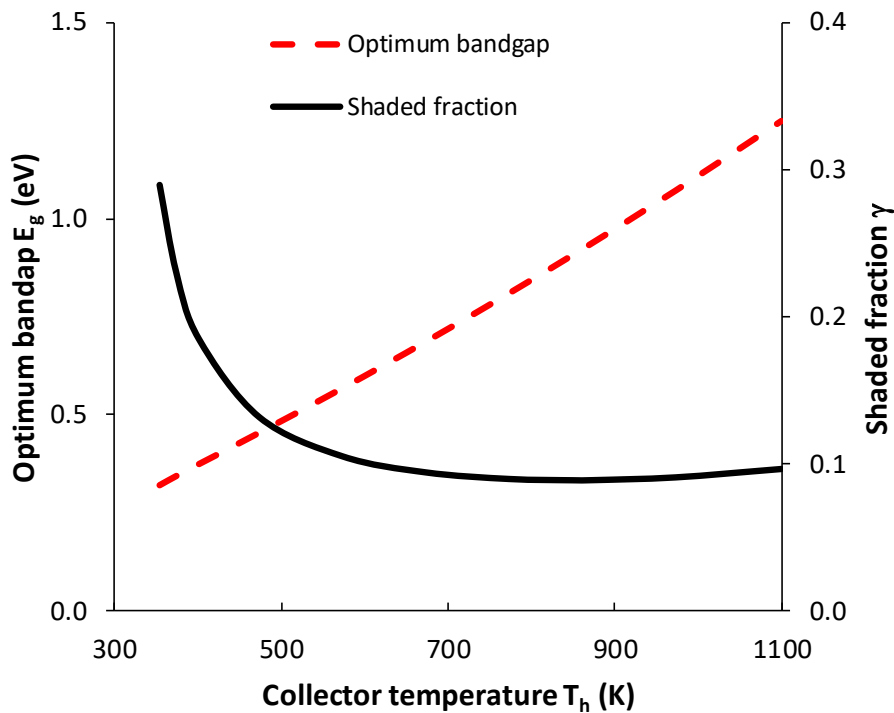
400  
 401  
 402 
$$\eta = \frac{1}{Cf\sigma T_{sun}^4} \frac{2\pi}{c^2 h^3} \int_{E_g}^{\infty} \left[ \frac{CfE^3}{\exp(E/kT_{sun}) - 1} + \frac{(1 - Cf)E^3}{\exp(E/kT_{sky}) - 1} - \frac{E^3}{\exp(E/kT_h) - 1} \right] dE$$
  
 403  
 404 (9).

405 Both  $E_g$  and  $T_h$  have to be optimized numerically to minimize  $\gamma$  (see Appendix B)  
 406 and the result at  $C=1$  is:  $E_g=0.91$  eV,  $T_h = 849$  K,  $COP = 12.5$  and  $\gamma = 0.089$   
 407 representing a considerable improvement on the previous value of  $\gamma=0.367$  for  
 408 the unselective collector. For the selective collector, increasing  $C$  also improves  
 409 performance eventually converging to the same minimum value of  $\gamma$  as without

410 the coating, since the optimized value of  $E_g$  tends to zero with increasing  $C$  – see  
411 Fig. 3<sup>32</sup>.

412

413 The collector with selective coating therefore seems more promising, even at  
414  $C=1$ , but its implementation could be hampered by availability of materials to  
415 withstand such high temperature of  $T_h = 849$  K (576°C). In case this temperature  
416 has to be limited to lower values, Fig. 4 shows that  $\gamma$  is not very sensitive to  $T_h$   
417 around the optimum, such that  $\gamma < 0.1$  is maintained at values down to  $T_h=615$  K  
418 (342°C), while at  $T_h=473$  K (200°C)  $\gamma=0.13$ . At 373K (100°C), however,  $\gamma$   
419 increases to 0.23.  
420



421

422

423 **Figure 4:** With a selective optical coating on the solar thermal collector ( $C=1$ ), blocking  
424 outgoing longwave radiation below the bandgap  $E_g$ , a minimum value of  $\gamma=0.089$  is  
425 obtained at  $T_h=849$  K increasing to  $\gamma=0.23$  at  $T_h=373$  K.  
426

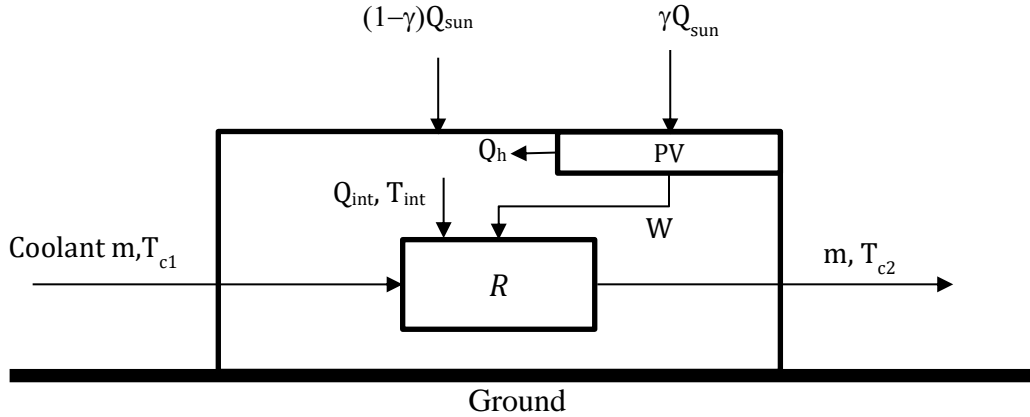
427

428

429

430 **5. Case of photovoltaic (PV) collector**

431



432

433

434 **Figure 5:** Case of the self-cooling greenhouse powered by a PV collector providing work  
 435 at rate  $W$  to a reversible refrigerator  $R$  and rejecting heat  $Q_h$  to the inside of the  
 436 greenhouse.

437

438

439 For the analysis of the PV collector (Fig.5), it is assumed initially that the  
 440 collector is housed inside the greenhouse, rejecting heat to the interior, and  
 441 operating at the internal temperature  $T_{int}$ . Like the thermal collector, it receives  
 442 solar energy at rate  $\gamma Q_{sun}$ . The efficiency of the PV collector  $\eta$  is defined in the  
 443 conventional way such that the work (i.e. electrical power) obtained from it is:

444

445

$$W = \eta \gamma Q_{sun} \quad (10).$$

446

447 We also define  $\lambda$  such that the PV collector rejects a certain amount of heat to the  
 448 interior of the greenhouse according to:

449

450

$$Q_h = \lambda \gamma Q_{sun} \quad (11).$$

451

452

453 This rejected heat adds to the heat to be removed by the refrigerator:

454

455

$$Q_{int} = Q_h + (1 - \gamma) Q_{sun} \quad (12).$$

456

457

458 Corresponding to the earlier entropy and enthalpy balances of eqs (1) and (2),  
 459 we obtain now:

460

461

$$\frac{Q_{int}}{T_{int}} = mc_p \ln \frac{T_{c2}}{T_{c1}} \quad (13)$$

462

463

and

464

$$W + Q_{int} = mc_p (T_{c2} - T_{c1}) \quad (14).$$

465 This time, with  $COP$  defined in the normal way for a mechanically driven  
 466 refrigerator as  $Q_{int}/W$ , we get the ideal value of:  
 467

$$468 \quad COP = \frac{1}{\bar{T}/T_{int} - 1} \quad (15).$$

469  
 470  
 471 Expressing heat and work flows in terms of  $Q_{sun}$  in the eqs. 10-12 above and  
 472 rearranging for  $\gamma$  gives:  
 473

$$474 \quad \gamma = \frac{1}{\eta COP + 1 - \lambda} \quad (16).$$

475  
 476  
 477 The values of  $\eta$  and  $\lambda$  are obtained by applying the detailed balance procedure to  
 478 the PV cell <sup>25</sup>. Like most PV devices available today, it is assumed to be of single-  
 479 junction type. At any photon energy level above the bandgap  $E_g$ , we can calculate  
 480 the net flow of photons converted into electrons based on the incoming flow of  
 481 solar photons, from which we subtract the outgoing flow according to Planck's  
 482 law modified by the bias voltage of the cell  $V$ . Once the net flow  $dN$  is calculated  
 483 for each small interval of wavelength  $dE$ , the total flow is integrated over the  
 484 entire spectrum from  $E_g$  to infinity:  
 485

$$486 \quad N = \frac{2\pi A}{c^2 h^3} \int_{E_g}^{\infty} \left[ \frac{CfE^2}{\exp(E/kT_{sun}) - 1} - \frac{E^2}{\exp([E - qV]/kT_{cell}) - 1} \right] dE \quad (17),$$

487  
 488  
 489 where  $c$  is the speed of light and  $h$  is Planck's constant. The outgoing flux  
 490 corresponds to radiative recombination which is an avoidable loss of solar cells.  
 491 The current is then obtained as  $I=Nq$  where  $q$  is the elementary charge. Finally,  
 492 the efficiency  $\eta$  is obtained by dividing by the work output  $W=IV$  by the total  
 493 power of the black body spectrum falling on the receiver, as given by Stefan's law  
 494  $ACf\sigma T_{sun}^4$ .  
 495

496 The calculation of  $\lambda$  is obtained from a similar detailed balance integration for  
 497 the energy flux of from the net absorbed photons after radiative recombination:  
 498  
 499

$$500 \quad Q_h = \frac{2\pi A}{c^2 h^3} \int_{E_g}^{\infty} \left[ \frac{CfE^3}{\exp(E/kT_{sun}) - 1} - \frac{E^3}{\exp([E - qV]/kT_{cell}) - 1} \right] dE \quad (18).$$

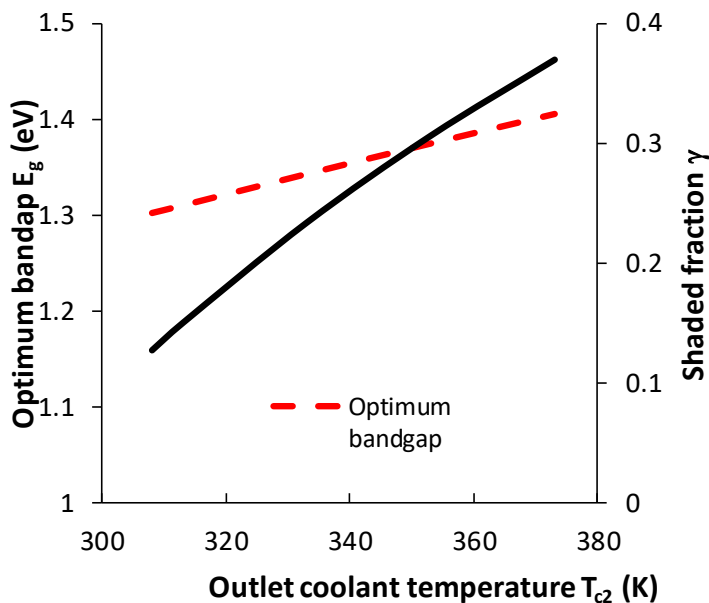
501  
 502 This allows the total energy absorbed by the solar cell to be calculated and then,  
 503 by subtraction of the work term  $W$ , we obtain  $Q_h$  and hence  $\lambda=Q_h/ACf\sigma T_{sun}^4$ . As  
 504 such,  $Q_h$  corresponds to thermalisation of carriers in the semiconductor from  
 505 their initial excitation energy (corresponding to the energy level of incoming  
 506 photons) to the energy level corresponding to the bias voltage  $V$  at which  
 507 electrical power is extracted. In the above,  $A$  is the area of the solar cell which  
 508 cancels out in the calculation of  $\eta$  and  $\lambda$ .

509 Note that, strictly speaking, there is also a contribution to  $N$  from the long wave  
 510 radiation corresponding to  $T_{sky}$  but this contribution is found to be negligible at  
 511 values of  $E_g$  of interest because long-wave radiation has much lower energy  
 512 levels and is assumed to be simply reflected from the solar cell after passing  
 513 through the semiconductor and bouncing off the back contact. Thus it does not  
 514 contribute significantly to either  $W$  or  $Q_h$ .

515  
 516 Minimisation of  $\gamma$  requires optimization of both  $E_g$  and  $V$  (see Appendix B).  
 517 Application of the above analysis to the baseline case (Table 1, at  $C=1$  and  
 518  $T_{c2}=313$  K) leads to optimal values of  $E_g=1.31$  eV,  $V=0.973$  V, resulting in  $COP$   
 519  $=19.6$  and  $\gamma=0.151$ , indicating that the minimum shaded fraction with a PV  
 520 single-junction cell as the power source is 15%.

521  
 522 The optimal bandgap of about  $E_g=1.3$  eV is the same as that already reported for  
 523 an optimized solar cell at  $C=1$  <sup>27</sup>. With increasing values of exit coolant  
 524 temperature  $T_{c2}$ , however, this value increases towards  $E_g=1.4$  eV (see Fig. 6).  
 525 This is because it is better to reduce the values of  $\lambda$ , and thus the additional  
 526 heating load on the greenhouse, favouring higher bandgaps and operating  
 527 voltages that minimize the thermalisation loss. The importance of this additional  
 528 load increases with  $T_{c2}$  which has the effect of decreasing  $COP$ . As these values of  
 529  $COP$  are idealized, real values are likely to be considerably lower, which would  
 530 favour higher  $E_g$  even at moderate values of  $T_{c2}$ . At a value of  $T_{c2} = 353$  K (80°C)  $\gamma$   
 531 increases to  $\gamma=0.307$  with optimal  $E_g=1.375$  eV. This confirms that, although  
 532 greater values of  $T_{c2}$  result in an economy of coolant fluid and associated  
 533 pumping power, they incur a penalty in the light entering the greenhouse for  
 534 photosynthesis because the solar collector has to be larger.

535

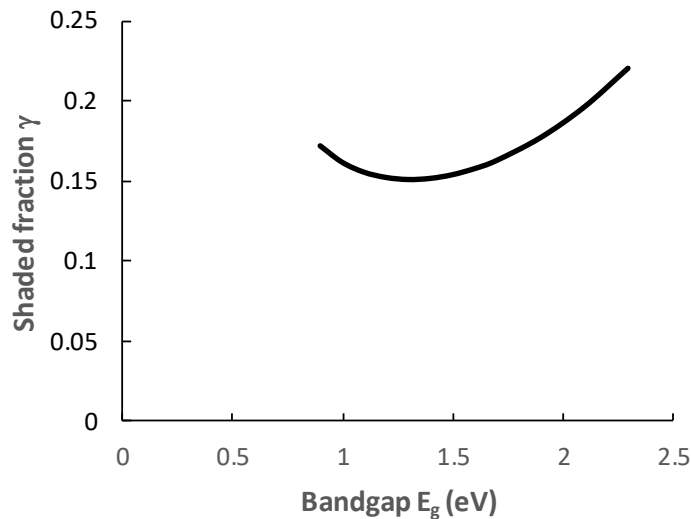


536  
 537 **Figure 6:** For the case of the PV self-cooling greenhouse, optimum bandgap  $E_g$  and  
 538 minimum shaded fraction  $\gamma$  both increase with outlet coolant temperature  $T_{c2}$ .

539  
 540



541 Whereas the above results indicate an optimum bandgap of about  $E_g=1.3$  eV, this  
 542 is not necessarily the preferred bandgap as it requires expensive semiconductors  
 543 in the III-V family<sup>43</sup>. Silicon is by far the most common material for solar cell  
 544 construction with  $E_g=1.1$  eV. Thus it is important to investigate the effect of  $E_g$  on  
 545 bandgap. Using eq.16 again, Fig.7 shows that the  $\gamma$  is not very sensitive to  $E_g$   
 546 remaining below 0.17 in the range  $E_g=1-1.7$  eV. Nonetheless, some organic PV  
 547 materials have considerably higher bandgaps e.g. 6,6-phenyl C61-butyric acid  
 548 methyl ester (PCBM) has  $E_g=2.3$  eV<sup>19</sup>. For this value, the minimum achievable  
 549 shading is increased from  $\gamma=0.15$  to 0.22 (Fig.7)

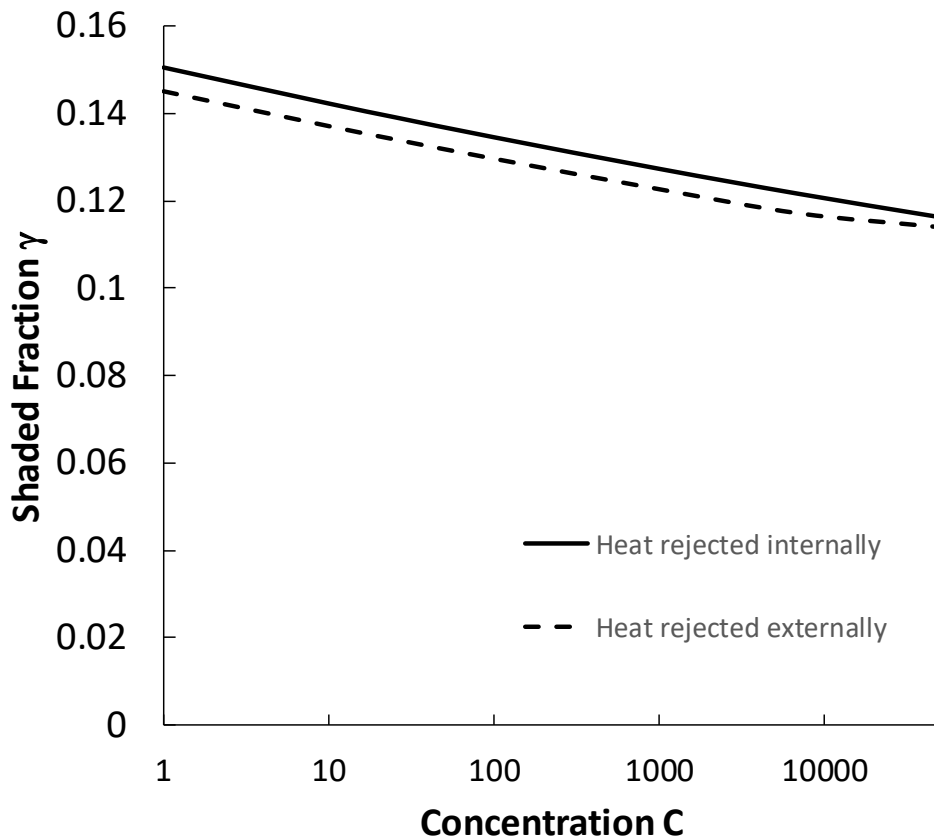


550  
 551 **Figure 7:** Effect of bandgap on minimum shaded fraction  $\gamma$  around the optimum of  
 552  $E_g=1.3$  eV for the solar PV collector.

553  
 554 The assumption in Fig. 5 and eq.(16), leading to the above results, is that the heat  
 555  $Q_h$  rejected from the PV collector entirely enters the greenhouse. This seems a  
 556 good assumption when the PV collector is internal to the greenhouse, as in the  
 557 studies of Li, Yano, Cossu, Yasunori, Matsuoka, Nakamura, Matsumoto and  
 558 Nakata<sup>17</sup> and Yano, Onoe and Nakata<sup>14</sup>. However, in other types of PV  
 559 greenhouse the collectors are integrated with the cladding<sup>19</sup>; or they could even  
 560 be mounted outside the cladding leaving an air gap. In the latter case, it would be  
 561 reasonable to assume that  $Q_h$  would not enter the greenhouse, and thus the term  
 562  $\lambda$  would be eliminated from eq.(16) causing  $\gamma$  to decrease from 0.151 to 0.143  
 563 with  $T_h$  kept at 293 K. On the other hand, with the PV collector outside the  
 564 greenhouse, its temperature  $T_h$  must increase as it cannot be cooler than the  
 565 surrounding air. Putting  $T_h=308$  K (35°C) increases  $\gamma$  from 0.143 to 0.145. Since  
 566 the value of  $\gamma$  is not therefore very sensitive to these assumptions, it is concluded  
 567 that  $\gamma=0.15$  is a reliable figure for the minimum shaded fraction in a single-  
 568 junction PV self-cooled greenhouse under the baseline conditions of this study.

569  
 570 Whereas the above calculations for the PV case are all for unconcentrated  
 571 sunlight ( $C=1$ ) it is well known that the efficiency of solar cells can be improved  
 572 under concentrated sunlight<sup>29</sup>. The resulting  $\gamma$  has been calculated here for a  
 573 range of concentrations for the cases of heat rejected both internally and  
 574 externally (Fig.8). Both cases show a decrease in  $\gamma$  by about 22% at the maximum  
 575 possible value of  $C=46300$  (ie. restoring the radiation to its intensity at the sun's

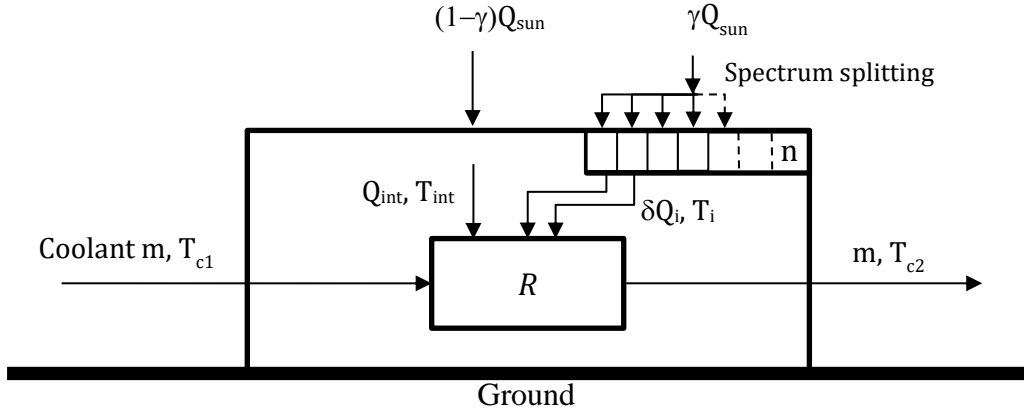
576 surface) where, for the parameter values in Table 1 and heat rejected internally,  
 577  $E_g=1.106$  eV,  $V=1.048$  V,  $COP=19.6$  and  $\gamma=0.116$ .  
 578



579  
 580  
 581 **Figure 8:** Effect of concentration ratio on the minimum shaded fraction  $\gamma$  using a single-  
 582 junction PV collector.

583  
 584  
 585 **6. Ultimate limit: case of multiple solar collectors with spectrum splitting**

586  
 587 De Vos <sup>36</sup> showed that an improvement to the single-temperature solar thermal  
 588 collector working at optimized temperature is obtainable by splitting the  
 589 incoming solar spectrum into many components of colour, with individual  
 590 collectors each optimized in temperature according to the incoming photon  
 591 energy level. It was also shown that the same analysis represents the limiting  
 592 performance of a multi-junction PV cell for an infinite number of junctions.  
 593 Although an infinite number of collectors or junctions cannot be practically  
 594 realised, this case is included here to represent the ultimate performance for any  
 595 solar-powered self-cooling greenhouse.  
 596



597  
598

599 **Figure 9:** Idealised self-cooling greenhouses using multicolour solar energy conversion  
600 via a large number  $n$  of collectors each at optimised temperature, representing an  
601 ultimate limit for both thermal and PV cases.

602  
603

604 We must now allow a series of heat sources to feed into the reversible thermally  
605 powered heat pump (Fig. 9) each one carrying its own heat and entropy flow.  
606 If there are in total  $n$  solar collectors, each receiving an amount of solar radiation  
607  $Q_i$  in the photon energy range  $E_i$  to  $E_i + \delta E$  according to Planck's law as:  
608

609

$$\delta Q_i = \frac{2\pi A}{c^2 h^3} \int_{E_i}^{E_i + \delta E} \frac{E^3 dE}{\exp(E/kT_{sun}) - 1} \quad (19).$$

610

611 Each one also loses blackbody radiation at the rate:

612

613

$$\delta Q_{i\_loss} = \frac{2\pi A}{c^2 h^3} \int_{E_i}^{E_i + \delta E} \frac{E^3 dE}{\exp(E/kT_i) - 1} \quad (20).$$

614

615 Maximum concentration corresponding to  $Cf=1$  has been assumed for this ideal  
616 limiting case. The efficiency of solar collection is calculated by subtracting  $\delta Q_{i\_loss}$   
617 from  $\delta Q_i$  and dividing by  $\delta Q_i$ . Thus each collector feeds heat at rate  $\eta_i \delta Q_i$  into  
618 the reversible machine at temperature  $T_i$ . The entropy and enthalpy and  
619 balances for the reversible machine will now be respectively:  
620  
621

622

$$\sum_i^n \frac{\eta_i \delta Q_i}{T_i} + \frac{Q_{int}}{T_{int}} = mc_p \ln \frac{T_{c2}}{T_{c1}} \quad (21)$$

623

624 and

625

626

$$\sum_i^n \eta_i \delta Q_i + Q_{int} = mc_p (T_{c2} - T_{c1}) \quad (22).$$

627

628 Combining the above two equations gives:

629

$$630 \quad \sum_i^n \delta Q_i \eta_i \left[ 1 - \frac{\bar{T}}{T_i} \right] = Q_{int} \left[ \frac{\bar{T}}{T_{int}} - 1 \right]$$

631

(23).

632 The amount of heat removed  $Q_{int}$  will be maximized when for each collector the  
 633 product  $\eta_i [1 - \bar{T}/T_i]$  is maximized by optimal choice of  $T_i$ . For the case of  $\delta E \rightarrow 0$   
 634 (infinitely many collectors) the collection efficiency becomes, as a function of the  
 635 receiver temperature  $T$ ,

636

$$637 \quad \eta(T) = 1 - \frac{\exp(E/kT_{sun}) - 1}{\exp(E/kT) - 1}$$

638

(24).

639

640 Defining  $COP$  with respect to the total solar heat flow to the solar collector, that  
 641 is as  $COP = Q_{int}/\gamma Q_{sun}$ , gives for the ideal case of infinitely many collectors:

642

$$643 \quad COP = \frac{1}{\sigma T_{sun}^4 (\bar{T}/T_{int} - 1)} \frac{2\pi}{c^2 h^3} \int_0^\infty \frac{\eta(T) [1 - \bar{T}/T(E)] E^3 dE}{\exp(E/kT_{sun}) - 1}$$

644

(25).

645

And from the overall heat balance according to this definition of  $COP$ :

646

$$\gamma = \frac{1}{1 + COP}$$

647

(26).

648 The analogy with the infinitely-many junction PV collector arises when the  
 649 temperature  $T(E)$  in the integral of eq.(25) is replaced with an effective PV cell  
 650 emission temperature  $T = \bar{T}/(1 - qV/E)$ , valid only under monochromatic  
 651 illumination<sup>44</sup>. This is very similar to the procedure used by De Vos to arrive at  
 652 the general result of 86.8% for the efficiency limit of both PV and solar thermal  
 653 multicolour conversion [De Vos<sup>36</sup>, Chapter 8]. By the same approach, we obtain  
 654 here identical values of  $COP$  and  $\gamma$  for these two cases. The 'planet temperature,  
 655  $T_p$ ' in the work of De Vos is replaced here by the logarithmic mean temperature,  
 656  $\bar{T}$ .

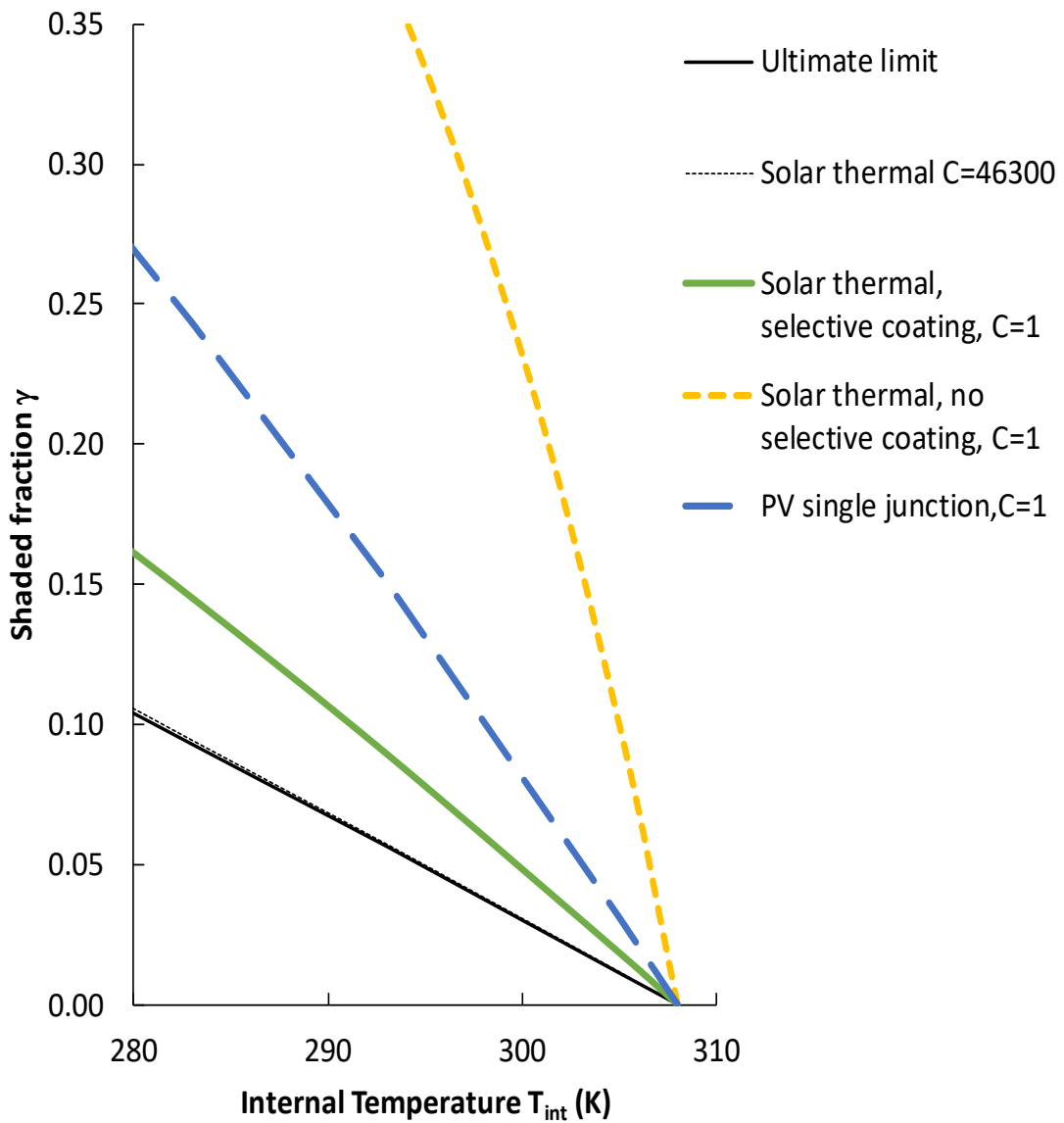
657

658 After the numerical calculation to optimise  $T(E)$ , maximising  $COP$  and  
 659 minimising  $\gamma$ , we obtain  $COP = 16.84$  and  $\gamma = 0.0561$ , just a marginal improvement  
 660 on the earlier value of  $\gamma = 0.0571$  for a single thermal collector at maximum  
 661 concentration. Nonetheless, this is less than half the value of  $\gamma = 0.151$  obtained in  
 662 the single-junction PV case.

663

664 The shaded fraction  $\gamma$  depends on the assumption about the internal  
 665 temperature, so far taken as  $T_{int} = 293$  K (20°C). However, different types of crops  
 666 may require different temperatures for cultivation, so it is important to  
 667 investigate the sensitivity of  $\gamma$  to  $T_{int}$  (Fig.10). With  $T_{int}$  decreased to 283 K (10°C)  
 668 the ultimate limit (i.e. multicolour collection) gives  $\gamma$  increased substantially from  
 669 0.0561 to 0.093. Fig.10 also includes results for the other types of solar collection

670 considered in this study, showing that  $\gamma$  generally increases significantly with  
 671 decreasing  $T_{int}$ .  
 672



673  
 674  
 675 **Figure 10:** Shaded fraction  $\gamma$  increases as internal temperature decreases, by a different  
 676 amount for each of the solar collector technologies considered.  
 677  
 678  
 679

680 **Table 2:** Summary of main results for the ideal minimum shaded fraction,  $\gamma$ , for different  
 681 types of solar collector - based on parameters in Table 1.  
 682

Type of solar collector	Modification	Solar concentration C	Collector temperature $T_h$ (°C)	Bandgap $E_g$ (eV)	Minimum $\gamma$
Thermal	None	1	92.5	NA	0.367
		46300	2206	NA	0.057
	Selective coating	1	576	0.91	0.089
		1	342	0.62	0.100
		1	100	0.35	0.230
PV (heat rejected into greenhouse)	NA	46300	2206	0	0.057
		1	NA	1.1	0.155
		1	NA	1.3	0.151
		1	NA	2.3	0.221
Ultimate limit (thermal and PV)	NA	46300	NA	1.1	0.116
		46300	NA	NA	0.056
		46300	NA	NA	0.056
		46300	NA	NA	0.056

683  
 684  
 685  
 686

## 7. Discussion

687 Table 2 summarises the main results for the minimum shaded fraction  
 688  $\gamma$  according to the different cases considered. Giving  $\gamma=0.15$ , the single-junction  
 689 PV self-cooling greenhouse seems only marginally promising, because the real  
 690 value of  $\gamma$  achievable is likely to be considerably higher on account of losses in  
 691 both the PV cell and the refrigeration machine it drives. Real PV cells have  
 692 efficiencies rarely exceeding two-thirds the thermodynamic maximum; and real  
 693 refrigeration machines have *COP* of perhaps half the Carnot limit. These factors  
 694 would increase  $\gamma$  to at least 0.4 by eq. (16). As noted in the Introduction, such a  
 695 high shaded fraction would likely reduce crop yield significantly.

696  
 697 On the other hand, improved future availability of multi-junction cells may make  
 698 the PV self-cooling greenhouse viable. At  $C=1$ , a two-junction cell has ideal  
 699 efficiency of 0.429, up from 0.31 for a single junction, reducing the ideal value of  
 700  $\gamma$  from 0.15 to about 0.11<sup>36</sup>. However, cost considerations in the proposed self-  
 701 cooling greenhouse are likely to be crucial, as greenhouse crops have to compete  
 702 with other modes of cultivation or imports from more temperate regions.  
 703 Therefore a low-cost and efficient multi-junction PV device would be needed,  
 704 unlike current commercial multi-junction devices which tend to be expensive.

705  
 706 As regards the solar-thermal self-cooling greenhouse, the simple blackbody  
 707 collector is very unpromising without optical concentration ( $C=1$ ) becoming  
 708 more feasible as  $C$  is increased above 10 (Fig.3). Sufficiently high concentration  
 709 ratios cannot be achieved with simple static arrangements; instead tracking  
 710 arrangements with at least one axis of motion would be required. Though this  
 711 would introduce some mechanical complexity, it is interesting to note that  
 712 Sonneveld, et al.<sup>45</sup> combined a static Fresnel lens with a tracking solar collector  
 713 (achieving  $C=25$ ) blocking out direct radiation and allowing only diffuse  
 714 radiation to reach the crops. According to the current study, the minimum  $\gamma$

715 possible at  $C=25$  is  $\gamma=0.12$  for a thermal collector without selective coating,  
716 decreasing to  $\gamma=0.08$  with selective coating; and  $\gamma =0.14$  for a PV collector (Fig.3  
717 and Fig.8 respectively). As an aside, we note that the collector studied by  
718 Sonneveld et al.<sup>45</sup> did not drive a refrigeration system, and was actually a hybrid  
719 photovoltaic-thermal collector. This hybrid case has not been considered here,  
720 and is an interesting case for future study.

721

722 According to the findings of this study, a solar thermal collector with selective  
723 optical coating appears promising, with  $\gamma=0.089$  achievable without the need to  
724 concentrate the sunlight. Solar thermal collectors could be used, for example, to  
725 power desiccant cooling systems<sup>46,47</sup>. Nonetheless, Fig. 4 shows that this can  
726 only be efficient if high temperatures ( $>250^{\circ}\text{C}$  say) are used in the solar thermal  
727 collection. Stationery, high-temperature ultra-vacuum solar thermal collectors  
728 have recently become available with operating temperature approaching  $200^{\circ}\text{C}$   
729<sup>48</sup>. This approach would also require high-temperature materials for use in the  
730 rest of the refrigeration system. Lefers, et al.<sup>49</sup> suggested an arrangement  
731 whereby solar-powered membrane distillation is used for regeneration of a  
732 liquid desiccant, with the additional feature that transpired water is recovered  
733 for irrigation. High temperature ceramic or polymer membranes may be  
734 developed in future for use in such systems.

735

736 For the sake of generality, some simplifying assumptions have been made in this  
737 study, concerning in particular the sky temperature  $T_{sky}$  which was set equal to  
738 the internal temperature  $T_{int}=293$  K. To check the validity of this assumption,  
739 different values of sky temperature have also been tried in the case of the solar  
740 thermal collector (without selective coating). For this purpose, eq.(5) is modified  
741 to include an additional term representing exchange of radiation with the sky.  
742 The calculations, detailed in Appendix A, confirm that for concentrations up to  
743  $C=1000$ , varying  $T_{sky}$  by  $\pm 10$  K affects the resulting  $\gamma$  by less than 5%.

744

745 This analysis is independent of the technological designs and materials and has  
746 been concerned only with a steady-state self-cooling greenhouse, neglecting any  
747 heat storage mechanisms. One contrasting example of a climate-controlled  
748 greenhouse for hot climates is offered by the *Watergy* project, which combined  
749 an internal heat exchanger with external reservoirs of water for heat storage  
750 allowing night-time cooling to be used<sup>50-53</sup>. This approach is particularly  
751 interesting for the Mediterranean climate, where substantial diurnal  
752 temperature swings occur. Extension of this analysis to consider supplementary  
753 night-time cooling is possible where good data on relevant ambient and perhaps  
754 sky temperature are available; however, the results will probably not be as  
755 general as they will depend on a larger number of input parameters.

756

757 Another topic for further study concerns the use of solar collectors that  
758 selectively allow certain spectral bands to pass into the greenhouse. An example  
759 of this proposed by Sonneveld, et al.<sup>54</sup> consisted of a greenhouse with a  
760 parabolic roof, providing a selective filter for photo-synthetically active radiation  
761 (PAR) while concentrating near-infrared (NIR) light for use in a solar collector of  
762 thermal, PV or hybrid type. The theory of blackbody absorbers could be  
763 extended to absorbers effective over different portions of the solar spectrum,

764 resulting in expressions for efficiency generally similar to eq.(9) but with the  
765 integrals applied piecewise. Thus selective transmission could be designed to  
766 match the photosynthetic action spectrum of the plants, allowing  $\gamma$  to be  
767 increased without sacrificing crop growth.

768  
769

## 770 **8. Conclusions**

771

772 This paper has shown the theoretical feasibility of self-cooling greenhouses. The  
773 fraction of light intercepted to drive the refrigeration system can be as small as  
774  $\gamma=0.056$  at the ideal thermodynamic limit. Such a small shaded fraction would  
775 not affect significantly the yield of crops. Nevertheless, this theoretical limit  
776 requires very complex, multicolour solar energy conversion to be implemented  
777 with many collection stages each optimised for a different portion of the solar  
778 spectrum and with the incoming sunlight concentrated maximally ( $C=46300$ ).

779

780 When more realistic concepts are considered, we obtain results ranging from  $\gamma$   
781  $=0.089$  for a thermal collector with a selective coating,  $\gamma=0.151$  for a single-  
782 junction PV cell, to  $\gamma=0.367$  for a thermal collector with no selective coating (in  
783 all cases without solar concentration,  $C=1$ ). The results are sensitive to the target  
784 temperature of the greenhouse interior,  $T_{int}$ . Thus, the above value of  $\gamma=0.089$   
785 obtained at  $T_{int}=20^\circ\text{C}$  increases to  $\gamma=0.12$  at  $T_{int}=15^\circ\text{C}$ .

786

787 In general, realisation of the self-cooling greenhouse requires advances in solar  
788 energy conversion and refrigeration technologies beyond the current state of the  
789 art. It could require, for example, integrated optical concentrators together with  
790 multi-junction PV devices, or thermal refrigeration systems driven at high  
791 temperatures, requiring considerable R&D effort for cost-effective and efficient  
792 incorporation of such techniques into horticultural greenhouses. Once initial  
793 prototypes of self-cooling greenhouses become available, it will be interesting to  
794 compare their performance against the results given here. Such comparisons  
795 could be made with the help of an exergy analysis.

796

## 797 **Acknowledgements**

798 The authors acknowledge support under the European Commission (DG for  
799 Research & Innovation) 7th Framework Program SFERA-II project for access to  
800 EU research installations (Grant Agreement n. 312643)

801

## 802 **Appendix A: Effect of sky temperature**

803

804 This appendix considers the sensitivity of the results to the assumption about  
805 sky temperature. Initially it was assumed  $T_{sky}=T_{int}$  such that radiation exchange  
806 between the greenhouse interior and the sky was negligible. When modified to  
807 include radiation exchange with the sky, eq.(5) becomes:

808

$$809 \quad Q_{int} = (1 - \gamma)[Q_{sun} + A_g \sigma (T_{sky}^4 - T_{int}^4)]$$

810

811 where  $A_g$  is the plan area of the greenhouse. The calculation for  $\gamma$  now gives, in  
812 place of eq.(7),



813

$$\gamma = \frac{1 + Z}{\eta COP + 1 + Z}$$

814

815 where

816

$$Z = \frac{1}{f} \left[ \frac{T_{sky}^4 - T_{int}^4}{T_{sun}^4} \right]$$

817

818 Use of which gives the following results for  $\gamma$  at different sky temperatures and  
 819 solar concentrations (solar thermal concentrator case without selective coating,  
 820  $T_{int}=293$  K):

821

	$T_{sky}=T_{int}=293$ K (baseline)	$T_{sky}=283$ K	$T_{sky}=303$ K
$C=1$	0.367	0.376	0.360
$C=30$	0.112	0.109	0.116
$C=100$	0.0907	0.0874	0.0943
$C=300$	0.0787	0.0758	0.0819
$C=1000$	0.0701	0.0675	0.0730

822

823 The results show a variation in  $\gamma$  of <5% with  $\pm 10$  K change in  $T_{sky}$ .

824

825

## 826 Appendix B: Optimisation methods

827

828 This appendix explains numerical details used in the various optimisation  
 829 calculations to minimise the value of  $\gamma$ . The Generalised Reduced Gradient (GRG)  
 830 method from the Solver toolbox of Excel® was used. For the case of the solar  
 831 thermal without coating (section 4.1) this method was used to optimise  $T_h$ . For  
 832 the case of the solar thermal with selective coating (section 4.2) the GRG method  
 833 was used to simultaneously optimise  $E_g$  and  $T_h$ . To calculate the integral in eq.(9),  
 834 the range of  $E$  was divided into 100 steps between  $E_g$  and  $E=3$  eV, then above 3  
 835 eV it was divided into 0.25 eV increments up to 8 eV where the integral was  
 836 truncated. Integration was done using the trapezium rule. For the case of the PV  
 837 collector (section 5) the GRG method was used to optimise variables  $E_g$  and  $V/E_g$   
 838 with eqs.(17) and (18) integrated similarly to above. For the PV collector with  
 839 multiple solar collectors (section 6) the values of  $T$  were optimised (again using  
 840 the GRG method) at each discrete value of  $E$  used in the numerical integration of  
 841 eq.(25). The convergence criterion for the GRG method was kept  $\leq 0.0001$   
 842 throughout. Results were verified against those available in reference <sup>36</sup> where  
 843 applicable.

844

845

846

847

848 **References**

849

- 850 1. WMO, Statement on the State of the Global Climate in 2017. In 2018.
- 851 2. PRB *World Population Data Sheet*; 2017.
- 852 3. Kumar, K.; Tiwari, K.; Jha, M. K., Design and technology for greenhouse  
853 cooling in tropical and subtropical regions: A review. *Energy and Buildings* **2009**,  
854 *41*, (12), 1269-1275.
- 855 4. Sethi, V. P.; Sharma, S. K., Survey of cooling technologies for worldwide  
856 agricultural greenhouse applications. *Solar Energy* **2007**, *81*, (12), 1447-1459.
- 857 5. Watt, J., *Evaporative air conditioning handbook*. Springer Science &  
858 Business Media: 2012.
- 859 6. Yang, S.-H.; Rhee, J. Y., Utilization and performance evaluation of a surplus  
860 air heat pump system for greenhouse cooling and heating. *Applied Energy* **2013**,  
861 *105*, 244-251.
- 862 7. Campen, J.; De Zwart, F.; Mohammed, A.; Ali, A.; Mohammed, D.,  
863 Climatisation of a closed greenhouse in the Middle East. In *GreenSys 2017*,  
864 *International Symposium on New Technologies for Environment Control, Energy-*  
865 *saving and Crop Production in Greenhouse and Plant Factory*, Beijing, 2017.
- 866 8. Puglisi, G.; Vox, G.; Schettini, E.; Morosinotto, G.; Campiotti, C., Climate  
867 Control Inside Greenhouses by a Means of a Solar Cooling System. In *GreenSys*  
868 *2017, International Symposium on New Technologies for Environment Control*,  
869 *Energy-saving and Crop Production in Greenhouse and Plant Factory*, Beijing,  
870 2017.
- 871 9. Lychnos, G.; Davies, P. A., Modelling and experimental verification of a  
872 solar-powered liquid desiccant cooling system for greenhouse food production  
873 in hot climates. *Energy* **2012**, *40*, (1), 116-130.
- 874 10. Ng, P. K.; Mithraratne, N., Lifetime performance of semi-transparent  
875 building-integrated photovoltaic (BIPV) glazing systems in the tropics.  
876 *Renewable and Sustainable Energy Reviews* **2014**, *31*, 736-745.
- 877 11. Cucchiella, F.; D'Adamo, I.; Koh, S. L., Environmental and economic  
878 analysis of building integrated photovoltaic systems in Italian regions. *Journal of*  
879 *Cleaner Production* **2015**, *98*, 241-252.
- 880 12. Kadowaki, M.; Yano, A.; Ishizu, F.; Tanaka, T.; Noda, S., Effects of  
881 greenhouse photovoltaic array shading on Welsh onion growth. *Biosystems*  
882 *Engineering* **2012**, *111*, (3), 290-297.
- 883 13. Pérez-Alonso, J.; Pérez-García, M.; Pasamontes-Romera, M.; Callejón-  
884 Ferre, A. J., Performance analysis and neural modelling of a greenhouse  
885 integrated photovoltaic system. *Renewable and Sustainable Energy Reviews*  
886 **2012**, *16*, (7), 4675-4685.
- 887 14. Yano, A.; Onoe, M.; Nakata, J., Prototype semi-transparent photovoltaic  
888 modules for greenhouse roof applications. *Biosystems Engineering* **2014**, *122*, 62-  
889 73.
- 890 15. Hassanien, R. H. E.; Li, M.; Yin, F., The integration of semi-transparent  
891 photovoltaics on greenhouse roof for energy and plant production. *Renewable*  
892 *Energy* **2018**, *121*, 377-388.
- 893 16. Castellano, S.; Santamaria, P.; Serio, F. J. J. o. A. E., Solar radiation  
894 distribution inside a monospan greenhouse with the roof entirely covered by  
895 photovoltaic panels. **2016**, *47*, (1), 1-6.

- 896 17. Li, Z.; Yano, A.; Cossu, M.; Yasunori, K.; Matsuoka, T.; Nakamura, H.;  
897 Matsumoto, T.; Nakata, J., Prototype Greenhouse Blind-type Shading System  
898 Using a Semi-transparent Photovoltaic Module. In *GreenSys 2017, International*  
899 *Symposium on New Technologies for Environment Control, Energy-saving and Crop*  
900 *Production in Greenhouse and Plant Factory*, Beijing, 2017.
- 901 18. Li, Z.; Yano, A.; Cossu, M.; Yoshioka, H.; Kita, I.; Ibaraki, Y., Electrical  
902 Energy Producing Greenhouse Shading System with a Semi-Transparent  
903 Photovoltaic Blind Based on Micro-Spherical Solar Cells. *Energies* **2018**, *11*, (7),  
904 1681.
- 905 19. Emmott, C. J.; Röhr, J. A.; Campoy-Quiles, M.; Kirchartz, T.; Urbina, A.;  
906 Ekins-Daukes, N. J.; Nelson, J., Organic photovoltaic greenhouses: a unique  
907 application for semi-transparent PV? *Energy & environmental science* **2015**, *8*,  
908 (4), 1317-1328.
- 909 20. Allardyce, C. S.; Fankhauser, C.; Zakeeruddin, S. M.; Grätzel, M.; Dyson, P. J.,  
910 The influence of greenhouse-integrated photovoltaics on crop production. *Solar*  
911 *Energy* **2017**, *155*, (Supplement C), 517-522.
- 912 21. Dupraz, C.; Marrou, H.; Talbot, G.; Dufour, L.; Nogier, A.; Ferard, Y.,  
913 Combining solar photovoltaic panels and food crops for optimising land use:  
914 Towards new agrivoltaic schemes. *Renewable Energy* **2011**, *36*, (10), 2725-2732.
- 915 22. Marcelis, L. F. M.; Broekhuijsen, A. G. M.; Meinen, E.; Nijs, E. M. F. M.;  
916 Raaphorst, M. G. M. In *Quantification of the growth response to light quantity of*  
917 *greenhouse grown crops*, 2006; International Society for Horticultural Science  
918 (ISHS), Leuven, Belgium: 2006; pp 97-104.
- 919 23. Thomas, M. D., Effect of ecological factors on photosynthesis. *Annual*  
920 *Review of Plant physiology* **1955**, *6*, (1), 135-156.
- 921 24. Blackman, F. F., Optima and Limiting Factors. *Annals of Botany* **1905**, *19*,  
922 (74), 281-295.
- 923 25. Shockley, W.; Queisser, H. J., Detailed balance limit of efficiency of p - n  
924 junction solar cells. *Journal of applied physics* **1961**, *32*, (3), 510-519.
- 925 26. Trivich, D.; Flinn, P., Maximum efficiency of solar energy conversion by  
926 quantum processes. *Solar Energy Research* **1955**, 143.
- 927 27. Araújo, G. L.; Martí, A., Absolute limiting efficiencies for photovoltaic  
928 energy conversion. *Solar Energy Materials and Solar Cells* **1994**, *33*, (2), 213-240.
- 929 28. Landsberg, P.; Mallinson, J. In *Thermodynamic constraints, effective*  
930 *temperatures and solar cells*, International Conference on Solar Electricity, 1976;  
931 1976; pp 27-42.
- 932 29. Henry, C. H., Limiting efficiencies of ideal single and multiple energy gap  
933 terrestrial solar cells. *Journal of applied physics* **1980**, *51*, (8), 4494-4500.
- 934 30. Marti, A.; Araújo, G. L., Limiting efficiencies for photovoltaic energy  
935 conversion in multigap systems. *Solar Energy Materials and Solar Cells* **1996**, *43*,  
936 (2), 203-222.
- 937 31. Markvart, T.; Bauer, G. H., What is the useful energy of a photon? *Applied*  
938 *Physics Letters* **2012**, *101*, (19), 193901.
- 939 32. Castañs, M., Bases físicas del aprovechamiento de la energía solar. *Revista*  
940 *Geofísica* **1976**, *35*, 227.
- 941 33. De Vos, A., Efficiency of some heat engines at maximum - power  
942 conditions. *American Journal of Physics* **1985**, *53*, (6), 570-573.

- 943 34. Jones, A.; Underwood, C., A thermal model for photovoltaic systems. *Solar*  
944 *energy* **2001**, *70*, (4), 349-359.
- 945 35. Adelard, L.; Pignolet-Tardan, F.; Mara, T.; Lauret, P.; Garde, F.; Boyer, H.,  
946 Sky temperature modelisation and applications in building simulation.  
947 *Renewable Energy* **1998**, *15*, (1-4), 418-430.
- 948 36. De Vos, A., *Thermodynamics of solar energy conversion*. John Wiley & Sons:  
949 2008.
- 950 37. Sørensen, B., *Renewable energy conversion, transmission, and storage*.  
951 Academic press: 2007.
- 952 38. Al-Subhi, A. M., Temporal and spatial distribution of the remotely sensed  
953 sea surface temperature in the northern Red Sea. *Journal of KAU-Marine Sciences*  
954 **2008**, *19*, (1).
- 955 39. Elliott, M. *Thermal standards for cooling water from new build nuclear*  
956 *power stations*; British Energy Estuarine and Marine Studies: 2011.
- 957 40. von Zabeltitz, C., Crop Growth Requirements and Climate Control. In  
958 *Integrated Greenhouse Systems for Mild Climates: Climate Conditions, Design,*  
959 *Construction, Maintenance, Climate Control*, von Zabeltitz, C., Ed. Springer Berlin  
960 Heidelberg: Berlin, Heidelberg, 2011; pp 29-43.
- 961 41. Rubin, M. H., Optimal configuration of a class of irreversible heat engines.  
962 I. *Physical Review A* **1979**, *19*, (3), 1272.
- 963 42. Müser, H. A., Thermodynamische behandlung von elektronenprozessen in  
964 halbleiter-randschichten. *Zeitschrift für Physik A Hadrons and Nuclei* **1957**, *148*,  
965 (3), 380-390.
- 966 43. Nelson, J., *The physics of solar cells*. World Scientific Publishing Co Inc:  
967 2003.
- 968 44. Davies, P.; Luque, A., Solar thermophotovoltaics: brief review and a new  
969 look. *Solar energy materials and solar cells* **1994**, *33*, (1), 11-22.
- 970 45. Sonneveld, P. J.; Swinkels, G. L. A. M.; Tuijl, B. A. J. v.; Janssen, H. J. J.;  
971 Campen, J.; Bot, G. P. A., Performance of a concentrated photovoltaic energy  
972 system with static linear Fresnel lenses. *Solar Energy* **2011**, *85*, (3), 432-442.
- 973 46. Davies, P. A., A solar cooling system for greenhouse food production in hot  
974 climates. *Solar Energy* **2005**, *79*, (6), 661-668.
- 975 47. Banik, P.; Ganguly, A., Performance and economic analysis of a  
976 floricultural greenhouse with distributed fan-pad evaporative cooling coupled  
977 with solar desiccation. *Solar Energy* **2017**, *147*, 439-447.
- 978 48. Calise, F.; d'Accadia, M. D.; Vicidomini, M.; Scarpellino, M., Design and  
979 simulation of a prototype of a small-scale solar CHP system based on evacuated  
980 flat-plate solar collectors and Organic Rankine Cycle. *Energy Conversion and*  
981 *Management* **2015**, *90*, 347-363.
- 982 49. Lefers, R.; Bettahalli, N. M. S.; Nunes, S. P.; Fedoroff, N.; Davies, P. A.;  
983 Leiknes, T., Liquid desiccant dehumidification and regeneration process to meet  
984 cooling and freshwater needs of desert greenhouses. *Desalination and Water*  
985 *Treatment* **2016**, *57*, (48-49), 23430-23442.
- 986 50. Zaragoza, G.; Buchholz, M., Closed greenhouses for semi-arid climates:  
987 Critical discussion following the results of the Watergy prototype. In *Acta*  
988 *Horticulturae*, 2008; Vol. 797, pp 37-42.
- 989 51. Buchholz, M.; Jochum, P.; Zaragoza, G., Concept for water, heat and food  
990 supply from a closed greenhouse -the watergy project. In *Acta Horticulturae*,  
991 2005; Vol. 691, pp 509-516.

- 992 52. Buchholz, M.; Buchholz, R.; Jochum, P.; Zaragoza, G.; Pérez-Parra, J.,  
993 Temperature and humidity control in the Watergy greenhouse. In 719 ed.; Acta  
994 Horticulturae: 2006; pp 401-408.
- 995 53. Zaragoza, G.; Buchholz, M.; Jochum, P.; Pérez-Parra, J., Watergy project:  
996 Towards a rational use of water in greenhouse agriculture and sustainable  
997 architecture. *Desalination* **2007**, *211*, (1), 296-303.
- 998 54. Sonneveld, P. J.; Swinkels, G. L. A. M.; Bot, G. P. A.; Flamand, G., Feasibility  
999 study for combining cooling and high grade energy production in a solar  
1000 greenhouse. *Biosystems Engineering* **2010**, *105*, (1), 51-58.  
1001